Probabilistic reliability assessment of existing masonry buildings: The church of San Justo y Pastor.

Fernando Ávila, Esther Puertas, Rafael Gallego*

Dept. of Structural Mechanics and Hydraulic Engineering, Universidad de Granada, Avenida Fuentenueva, 18001 Granada, Spain

Abstract

There exists a large number of masonry historical buildings with a high heritage value whose preservation has to be ensured. For this purpose, it is important to establish a methodology to assess their structural reliability in the case of extraordinary load events. Particularly, the materials and construction techniques employed in this kind of buildings make them especially vulnerable in the event of an earthquake.

This paper presents and discusses a probability-based reliability analysis to determine the damage on existing masonry structures subjected to seismic loads. Geometric and material data are introduced in a three-dimensional FEM model, which takes into consideration the uncertainties that exist in the material properties. The reliability of the structure is determined via the definition of a Damage Index and carrying out a Monte Carlo-type analysis. The case of study presented in this paper is the church of San Justo y Pastor located in Granada, a seismic-prone region in southern Spain.

Keywords: masonry historical buildings, probabilistic assessment, reliability assessment, seismic damage, FEM analysis

1. Introduction: objectives and methodology

The Church of San Justo y Pastor is a relevant masonry construction within Granada's architectural heritage, built by the Jesuits between the 16th and 18th centuries [1, 2] (Figure 1). This paper presents an architectural and geometrical analysis of the church and a structural reliability assessment of its bell tower, found as the most vulnerable feature, in the event of an earthquake.

In order to conduct the architectural and geometrical analysis, an exhaustive bibliographic research is needed. Taking into account the information obtained from several books and treatises about Jesuitical architecture [1, 2, 4] and the

*Corresponding author

Email addresses: favila@ugr.es (Fernando Ávila), epuertas@ugr.es (Esther Puertas), gallego@ugr.es (Rafael Gallego)

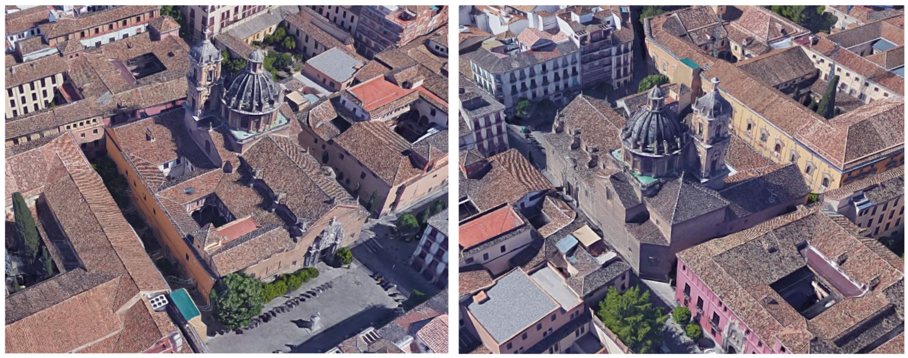

Figure 1: Church of San Justo y Pastor, aerial views [3].

blueprints of projects developed in the church and still kept in archives [5], it is possible to define the structure of the building and reproduce it in a three-dimensional Finite Element (FE) model.

Once the geometrical model is created, it has to be provided with the properties of the materials present in the church, which are mainly travertine and calcarenite [6]. Considering the difficulty in obtaining samples to evaluate the material properties in a historical structure [7], these mechanical properties can be obtained by testing the walls of the church using non-destructive techniques [8]. However, significant uncertainties in their values are always present due to the measurement procedure, the deviation in the characteristics of heterogeneous materials (intrinsic or related to alteration in time) and the lack of completeness in the variables considered in the model [9]. In these cases, a probabilistic analysis provides a significant advantage, since it defines statistically the material properties through probabilistic distributions with controlled parameters, following a Monte Carlo type approach [10].

The probabilistic analysis that is carried out is the basis for a reliability assessment of the church when subjected to a seismic event according to the seismicity of the location. Since historical stone-masonry structures are particularly vulnerable to earthquakes due to their high weight and small tensile strength, and bearing in mind that they were built at a time when seismic risk was not formally considered in structural design [11], this analysis provides useful information in order to take measures, if necessary, to protect and preserve them. It is even more relevant taking into account that this kind of buildings is particularly valuable and that they are usually placed in busy areas of the cities, with the consequent potential loss of life and property.

1.1. Structural reliability: applicability and review

Over the last decades, the concepts of limit and serviceability states, and safety requirements have been widely developed and included in the design codes in Europe and North America, but the focus has always been on the design of new structures [12]. However, several structural collapses have occurred in historical buildings [13], showing the vulnerability of the cultural and historical heritage and revealing the need to apply the concepts of safety, reliability and hazard to the existing constructions. The existing structural codes, developed for the construction of new structures, are often inadequate for existing buildings [14], being necessary a specific methodology for this kind of buildings.

To face the problem of evaluating the structural capacity of an existing structure, some non-normative manuals and codes have been developed over the last years, either with a general approach or focused on masonry structures [11, 14–16]. In general terms, six assessment levels can be distinguished [14]:

- Level 0. Non-formal qualitative assessment.
- Level 1. Measurement based determination of load effect.
- Level 2. Partial factor method, based on document review.
- Level 3. Partial factor method, based on supplementary investigation.
- Level 4. Modified target reliability, modification of partial factors.
- Level 5. Full probabilistic assessment.

These levels go from a mere subjective visual analysis to a full probabilistic analysis. In this highest level of assessment it is possible to evaluate the probability of failure of a structure, and quantify its reliability under the effect of certain actions, which can be also subjected to a probabilistic distribution.

Structural reliability methods are particularly interesting when evaluating a seismic action, as this is one of the main threats for the integrity of historical constructions [17–19].

2. Historical context. The church of San Justo y Pastor

In the middle of the 16th century, the Jesuit order arrived to Granada. After a first location in Abenamar St, they decided to move to a bigger place in order to build a greater complex, which would be called Saint Paul's College. The chosen place was beside the city walls, near the door of San Jerónimo, and the complex would have three differentiated spaces: the Residence, the Schools and the Church.

The works started on May 26th, 1575 [1] following the original idea of the architect P. Bartolomé Bustamante, but the project was later modified by Juan de Maeda, who considered more suitable to use blocks of travertine instead of the original bricks. The works began under the direction of the Jesuit Martín de Baseta and the supervision of Lázaro de Velasco. Fourteen years later, in 1589, the main nave and the lateral chapels were finished [2]. The church was inaugurated with dedication to Saint Paul.

During the last years of the 16th century and the beginning of the 17th, a side entrance and a sumptuous dome, designed by Br. Pedro Sánchez under the supervision of Br. Alonso Romero, are built. These works were finished in 1622.

Two of the most representative elements of the church, the bell tower and the main façade, were built almost a century later. The tower was designed by the architect José de Bada, who won a contest organised to that effect, and was completed in November 1719 [2]. This masonry tower has three superimposed bodies with square cross-section topped by a faceted dome. The main façade (Figure 2) was built some years later, between 1738 and 1740, by the priest Francisco Gómez, and it has two different bodies of columns, a semi-circular arch and reliefs of white marble [20].

Figure 2: Main and lateral façades and dome of the church of San Justo y Pastor.

In the second half of the 18th century, the Jesuit order was expelled from Spain and the church was closed at first for 4 years. Later on, it was used as the see of the *Colegiata del Salvador* and finally, in 1799, it became the parish of San Justo y Pastor, a denomination that retains to this day [4].

Over the following years, few changes were made in the building. There were only two remarkable interventions: the separation between the church and the convent of *La Encarnación* (in 1835) and the restoration project by the architect J. A. Llopis Solbes in 1981, aimed to solve the serious water infiltrations in the roof and dome of the church [5]. One year before this project, the church was declared a Cultural Heritage Asset by the Spanish Government [21].

3. Architectural and geometrical analysis

3.1. Architectural description and general characteristics

The church of San Justo y Pastor has a single central nave and side chapels (Figure 3); the nave and the transept define a Latin cross layout, even though the plan of the complete building is rectangular. This provides to the building a plain external appearance where only the main façade, the bell tower and the dome stand out as ornamental elements.

The design of this church shows relevant innovations in the Andalusian ecclesiastical architecture of the 16th century, being the first church in Granada

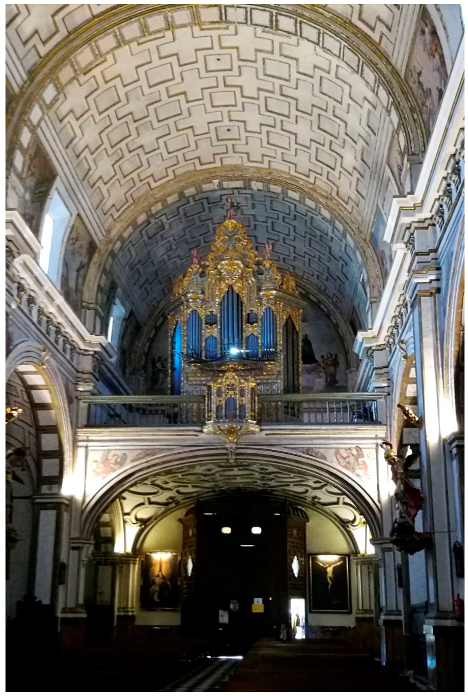

Figure 3: Main nave of the church of San Justo y Pastor, interior view.

that expresses the Counter-Reformist ideas. Also the incorporation of the side chapels to the nave is an innovation compared to the previous Andalusian churches, changing the Jesuitical concept of liturgical exclusivity of the church in order to introduce support from individuals via these chapels [2, 22].

3.2. Definition of geometry

The available information referring to the geometry of the church of San Justo y Pastor is scarce, mainly because most of the documents of the Jesuits were lost or destroyed after they were expelled in 1767. Regarding the plan of the building, the only original blueprints are two anonymous drawings made in 1579 and preserved nowadays in the Spanish National Historical Archive [23]. More accurate information is obtained from the blueprints developed by the architect J. A. Llopis Solbes for the restoration project in 1981, shown in Figure 4. According to this project [5] and the information compiled by Córdoba Salmerón [2], the following geometrical data are deduced:

- Rectangular plan with dimensions 46.5 m × 21.5 m and 1.0 m-thick stone-masonry walls. The north corner of the building is chamfered at a 45° angle.

- The six lateral chapels, three on each side, have inner dimensions 7.0 m × 3.9 m. The main chapel, located in the apse, is 10.3 m long and 8.6 m wide.

- The transept has inner dimensions 19.5 m × 10.3 m.
- The front of the building is 19 m high at its central and highest point, and 10.2 m high on the sides. All the façades have several windows, standing out the sides of the ones placed at both ends of the transept.
- The main entrance, which faces the University Square, is 3 m wide and 5 m high at the central point of its semi-circular arch. The side entrance, at San Jerónimo St, is a 3 m × 5 m rectangle.

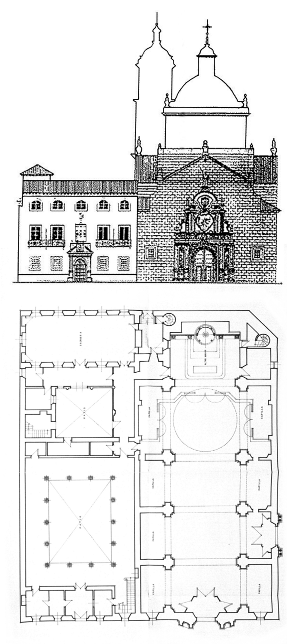

Figure 4: Floor plans and elevations of the church of San Justo y Pastor and the adjacent cloisters [5].

With regard to the dome, more detailed information is available thanks to the field measurements carried out by Ramírez Molina [6]. The hemi-spherical dome has 9 m inner diameter, 6 m height and a variable thickness between 50 cm at its base to 7 cm at the top. The dome rests on a tambour of 10 m inner diameter and 1 m-thick masonry walls. Crowning the dome there is a 2 m-diameter cylindrical lantern, 3 m high. The top of the lantern is at a height of 34.8 m above the pavement level.

Over the nave and the transept, barrel vaults are placed. Considering the aforementioned references for the dome and the common characteristics of this kind of vaults in churches of the same period, their geometry can be defined in quite an accurate way. The vaults have a semi-cylindrical body with inner diameter 10 m and thickness 50 cm. In correspondence with the pillars the vault is reinforced with semi-circular lunettes.

The last main element to be geometrically described is the bell tower. It has three square-plan bodies. The first one is 19.5 m high with a side length of 5.7 m, the second one has the same cross-section and is 7.5 m high while the third one is 5.5 m high with a 5 m-side square cross-section. This last body is the one where the bells are placed.

Considering the geometrical description above, it is possible to design the complete blueprints of the church, adopting a simplified geometry that accurately represents the structural behaviour of the building (Figure 5). This is the basis for the 3D model used in the structural analysis.

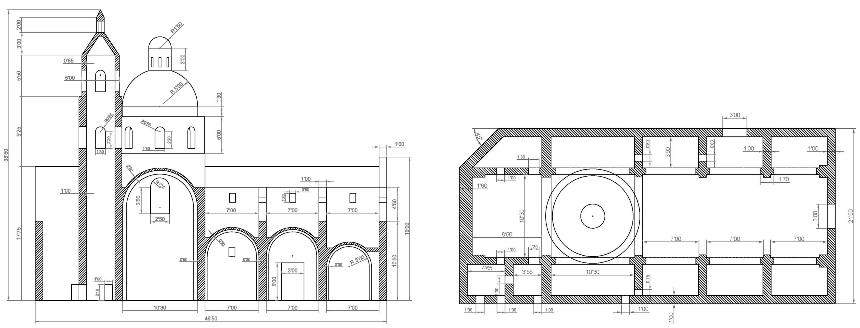

(a) (b)

Figure 5: Longitudinal section along the side chapels (a) and plan view (b) of the simplified model of the church.

4. Analysis of materials

According to the historical documentation and the subsequent verifications [6, 24], there are two materials that constitute the church of San Justo y Pastor: travertine and calcarenite.

Travertine comes from the quarry of Alfacar (Granada), and it was used in the construction of most of the church: walls and pillars, bell tower and tambour of the dome. This is a porous sedimentary rock with a good performance against water and a notable mechanical strength [25]. The calcarenite of Santa Pudia, on the other hand, is a calcareous rock with a high presence of bioclasts and with a grain size similar to the sand (20 µm to 2 mm). These properties make calcarenite easy to extract from quarry and enhance its workability, but render it mechanically weak.

The material mechanical properties where determined by Martínez-Soto and Gallego [24] via Spectral Analysis of Surface Waves (SASW) [8]. The data obtained via this non-destructive method are the base values for the density, static and dynamic Young's modulus, dynamic shear modulus and Poisson's ratio, as shown in Table 1.

The compressive strength of the materials can be estimated via empirical formulations from various authors and codes, as suggested by García Marín [24]. The final value considered for the compressive strength is the mean of the individual results, eliminating first the two extreme values. The results are collected in Table 1.

- ACI Committee 318 [26]:

$$E_d \text{ [GPa]} = 4730 \sqrt{f_c}$$

- ACI Committee 318S [27]:

$$E_s \text{ [MPa]} = 40.043 \, \rho^{1.5} \sqrt{f_c}$$
$$E_d \text{ [MPa]} = \rho^{1.5} \left(0.024\sqrt{f_c} + 0.12\right)$$

- ACI Committee 363 [28]:

$$E_d \text{ [MPa]} = 3320 \sqrt{f_c} + 6900$$

- Eurocode 2 [29]:

$$E_s \text{ [GPa]} = 22 \left(f_c/10\right)^{0.3} \left(\rho/2200\right)^2$$

- Yildirim and Sengul [30]:

$$E_s \text{ [GPa]} = 5.58\sqrt{f_c} - 13.5$$

where E_s and E_d are, respectively, the static and dynamic Young's modulus, f_c is the compressive strength in MPa and ρ is the material density in kg/m^3. It should be noted that these are statistical correlations between the average values of material properties, but they do not hold exactly in specific samples.

With regard to the tensile strength, the values proposed for masonry by the FEMA [31] and the JCSS [32] are adopted, leading to a value of the tensile strength equal to $f_t = 1.0\,\text{MPa}$.

4.1. Probabilistic distribution of material properties

The probabilistic reliability assessment is based on introducing a probabilistic distribution for those variables of the problem that are subjected to stochastic phenomena or whose determination entails uncertainty, as is the case with ancient masonry material properties [33]. With this kind of probabilistic approach, the randomness in the model parameters is explicitly considered and thus the structure reliability can be quantitatively assessed [34].

As indicated in the JCSS Probabilistic Model Code [32], the base values of the main material properties (compressive and tensile strength and Young's modulus) obtained from the SASW are multiplied by random variables, x_i, following a log-normal probabilistic distribution. The use of this kind of distribution is recommended for the evaluation of reliability and probability of failure because [35]:

Parameter	Travertine	Calcarenite
ρ [g/cm^3]	1.81	1.85
E_s [GPa]	19.93	18.68
E_d [GPa]	23.95	22.84
G_d [GPa]	8.60	8.84
ν [–]	0.39	0.29
f_c [MPa]	29.40	26.61
f_t [MPa]	1.00	1.00

Table 1: Base values for the materials mechanical properties.
ρ: density; E_s: static Young's modulus; E_d: dynamic Young's modulus; G_d: dynamic shear modulus; ν: Poisson's coefficient; f_c: compressive strength; f_c: tensile strength.

- It assigns probability zero to all negative values of the variable, so the probability of failure is never negative.

- As it depends on two parameters, mean and variance, it fits easily with a wide range of empirical distributions.

- Its mean is greater than its median, so it places greater importance on the highest values of failure than a normal distribution with the same percentiles of 5 % and 50 %, which means that it is a more "pessimistic" or "cautious" distribution.

The probability density function for a log-normal distribution is:

$$f(x) = \frac{1}{x\sigma_y\sqrt{2\pi}} \exp\left[-\frac{(\ln x - \mu_y)^2}{2\sigma_y^2}\right]$$

where $x > 0$, and μ_y and σ_y are the mean and standard deviation, respectively, of the associated normal distribution $y = \ln x$. According to JCSS [32], the log-normal distributions of the variables x_i have a mean (μ) equal to 1 and Coefficient of Variation (CV) of 15 % for compressive strength, 25 % for Young's modulus and 30 % for tensile strength.

The probability density functions and cumulative probability distributions for each parameter of both materials are shown in Figure 6.

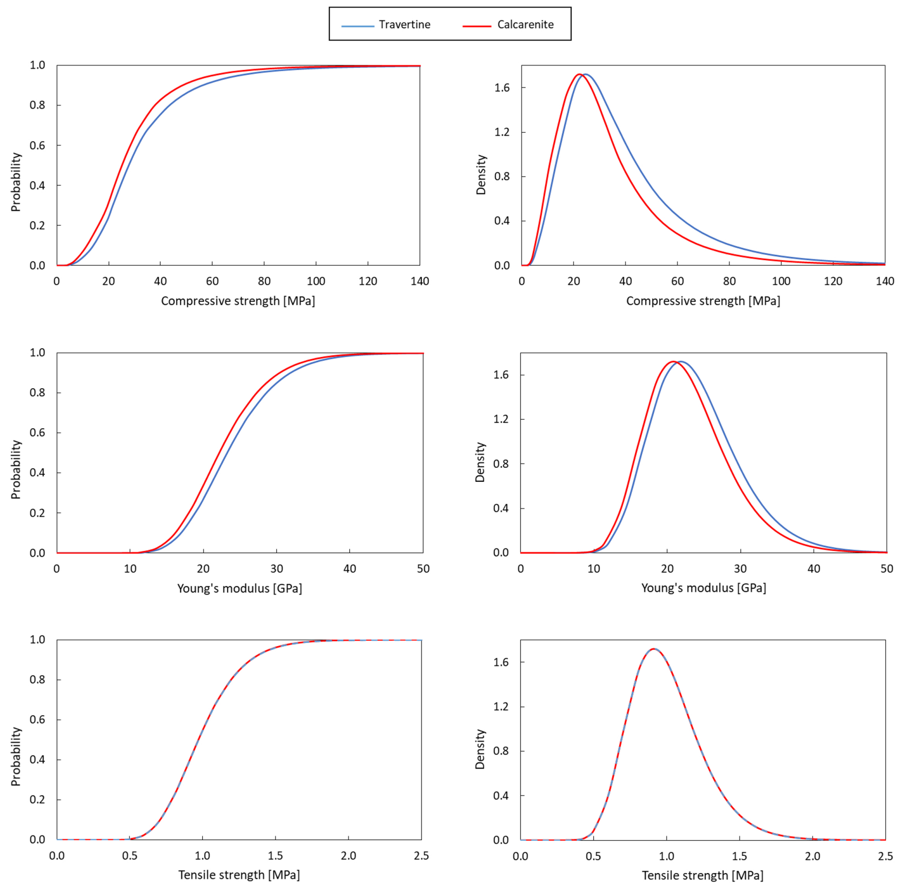

Figure 6: Cumulative probability distributions (left) and probability density functions (right) of travertine and calcarenite mechanical properties.

5. Probabilistic reliability analysis

5.1. Methodology of the analysis

Monte Carlo method is used to estimate the probability of failure, considering the problem as a series of N deterministic calculations, where each calculation i is performed with different input values (material properties) defined by probability distributions. This method is useful for the reliability assessment due to its ability to provide reliability indexes using analytical techniques, not requiring extra formulation, even though it is computationally expensive [10].

According to this description, the steps for the calculation are listed below, leading to the workflow diagram in Figure 7:

Step 1. Material properties (compressive strength, tensile strength and Young's modulus) for both materials are selected, according to their log-normal distributions.

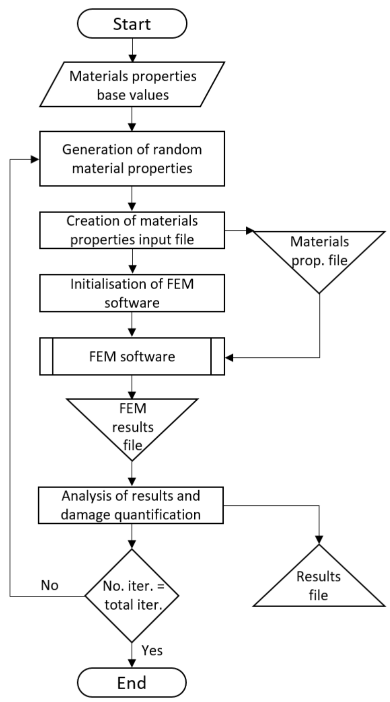

Figure 7: Probabilistic reliability assessment methodology workflow.

Step 2. These material properties are introduced in the FE model.

Step 3. The problem is solved under the action of the self-weight of the structure and a seismic event.

Step 4. The damage is assessed following the chosen criterion (described below).

Step 5. The results are saved and the whole process is repeated until N computations are completed.

The values of compressive strength and Young's modulus are chosen independently in Step 1, since the statistical correlation that exists between them is taken into account when selecting the averages of their probability distributions.

To assess the reliability of the structure, a Damage Index (DI) is defined as the ratio between the damaged volume and the total volume of the structure, in percent, as suggested by Asteris et al. [36]:

$$DI\ [\%] = \frac{V_{\mathrm{damaged}}}{V_{\mathrm{total}}} \times 100$$

With this quantitative index as a basis, three structural performance levels are defined, in order to express qualitatively the state of the structure after the seismic action. These performance levels are established following the recommendation for masonry in FEMA 356 [31] and are adopted by Asteris et al. [36] as well:

- Insignificant Damage ($DI < 15\,\%$): minor superficial cracking and minor spalling at corners. No observable out-of-plane offsets.
- Moderate Damage ($15\,\% \leq DI < 25\,\%$): generalized cracking and perceptible in-plain offsets of masonry. Minor out-of-plane offsets.
- Heavy Damage ($DI \geq 25\,\%$): generalized cracking. Significant in-plain and out-of-plane offsets.

In order to compute the total damaged volume, it is considered that an element fails when the material elastic limit is exceeded. This can be quantified by registering the Equivalent Plastic Strain variable in the FE model.

5.2. FEM modelling

In order to carry out the analysis, the first step consists of creating a 3D model of the church from the defined geometrical data. This model is introduced in a Finite Element Method (FEM) software where the material properties, loads and boundary conditions are included. The FE model of the church, shown in Figure 8, has 155 374 elements, 230 950 nodes and 692 850 degrees of freedom. The mesh size is defined according to a sensitivity analysis carried out to determine the influence of the mesh density. The mesh size was defined computing the first three natural frequencies using meshes with increasing element densities until convergence.

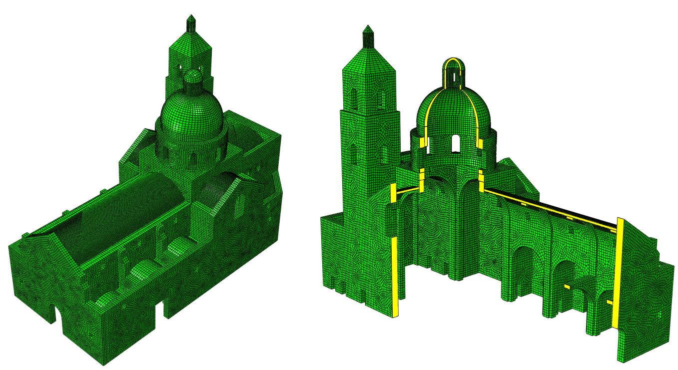

Figure 8: FEM model of the building. General view (left) and 90° section (right).

The behavior of the masonry materials is represented via macro-modelling, which is a common approach to analyze large structural members or full structures, as is the case of this paper, due to its lower computing time requirements and its adequate approach for the characterization of the structural response. It has been widely use to analyze the seismic response of masonry buildings [37].

The non-linear behavior of masonry has been modeled using the Concrete Damage Plasticity (CDP) model. Even though this material model was originally designed for concrete [38], it has been frequently used to represent the mechanical behavior of other quasi-brittle material with a certain degree of anisotropy by adapting its parameters [39–43]. In addition, the CDP model is particularly appropriate for calculations where the material is damaged under loading-unloading cycles and for dynamic analysis [38, 44]. In this model, the axial compression response of the material is linear until the yield stress is reached, followed by hardening before compression crushing initiates (Figure 9a). The behavior in tension is considered linear elastic up to the tensile stress peak, where micro-cracks start to propagate and the stress-strain curve drops down following a softening branch (Figure 9b). Additional parameters needed to define the CDP model are obtained from literature [40, 41, 44, 45] as shown in Table 2.

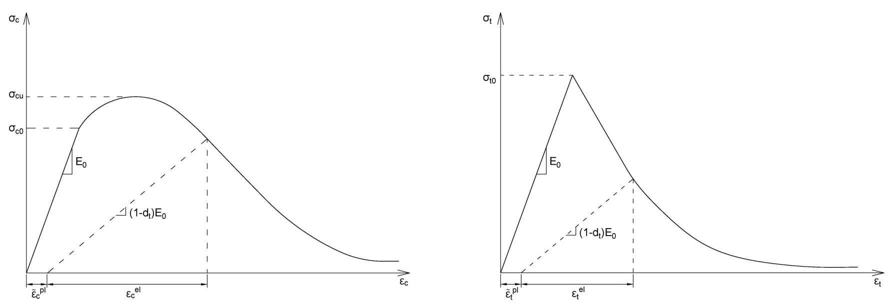

(a) (b)

Figure 9: Mechanical behaviour of masonry under uniaxial compression (a) and tension (b) in CDP model.

Parameter	Value
Dilation angle [°]	12
Eccentricity	0.1
f_{b0}/f_{c0}	1.16
K_c	0.667
Viscosity parameter	$9 \cdot 10^{-4}$

Table 2: Concrete Damage Plasticity parameters adopted for masonry in the numerical simulations.

The building is meshed with 8-node linear elements with continuum stress-displacement and reduced integration. They are all hexahedral elements except for the dome and the roof of the bell tower, where tetrahedrons are used due to the more complex geometry. The average mesh size is 0.35 m, being smaller in the lantern, dome and vaults.

Two different loads are included in the model to perform the calculation:

the self-weight of the building and a seismic acceleration in both horizontal directions.

5.2.1. Seismic acceleration

The location of the church of San Justo y Pastor, the South-East of the Iberian Peninsula, is one of the zones in Europe with the highest seismic hazard [46]. The seismic hazard for the specific location is determined by the Spanish seismic code [47], which gives a basic seismic acceleration equal to 0.23 g for a return period of 500 years.

According to the aforementioned standard [47], the category of the building and the type of soil have to be taken into account, along with the basic seismic acceleration, to obtain the basal acceleration. Considering the high heritage value of the church, it can be cataloged as a construction "of special interest". The soil is compounded of old alluvial materials, mainly clay and silty sand with minor gravel layers [48], which leads to a Type-III soil, according to the seismic code. With these parameters the basal seismic acceleration is 0.33 g, which will be used as the Peak Ground Acceleration (PGA) for the reliability analysis.

The accelerogram used for the calculation belongs to a seismic event happened in L'Aquila (Italy) on April 2009 and whose characteristics are similar to a potential earthquake that may occur in the location of the church [49]. From the original seismic event, with a total duration of ca. 15 s (Figure 10), only the 2.50 s range with the highest intensity is chosen for the analysis in order to reduce the computational cost. The accelerogram is also scaled to reach the PGA of 0.33 g and spline-refined to interpolate it every 0.002 s.

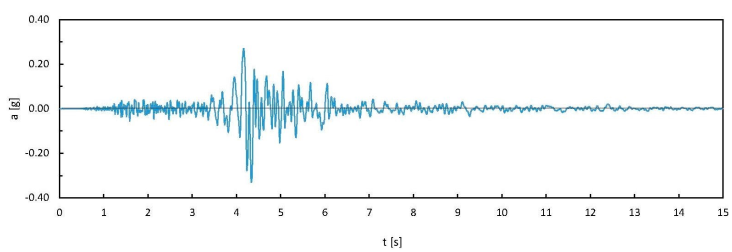

X direction

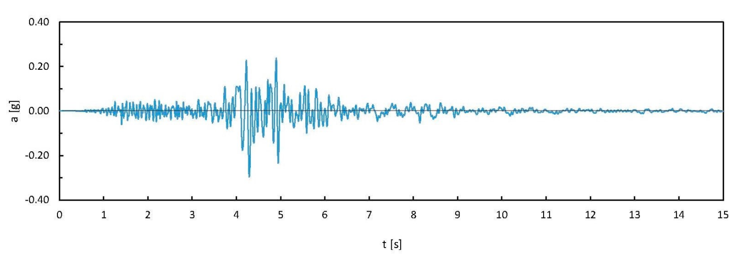

Y direction

Figure 10: Accelerograms used for the dynamic analysis.

5.3. Analysis of results

As a first step in the calculation, the church is subjected to the dynamic action with material properties equal to their base values shown in Table 1. The results in Figure 11 reveal that the main body of the church behaves as a quasi-rigid body compared to the bell tower, which undergoes larger displacements. This situation generates a significant stress increase in the tower, especially in its union with the church walls, making the bell tower the most vulnerable zone in the case of an earthquake. Recent studies on damage assessment of masonry churches [33, 50] have also found that bell-gables and bell towers are the most vulnerable elements in the case of a seismic event.

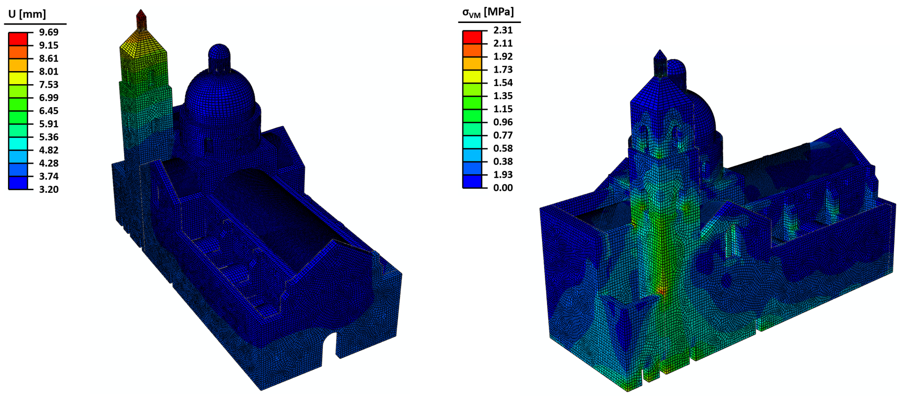

(a) (b)

Figure 11: Contour plots of displacements (a) and Von Mises stresses (b) in the church under seismic action.

Taking into account these global results, an isolated model of the bell tower is created in order to carry out the probabilistic analysis. The union between the tower and the main body of the church is considered fixed due to the high stiffness of the junctions. The analysis is performed according to the methodology described in the previous subsections, carrying out a total of 1000 simulations. This number of simulations is enough to attain convergence in the mean value and standard deviation of the output (Damage Index), as shown in Figure 12.

In addition, to ensure that the number of simulations is enough to give a meaningful average and distribution of performance, the frequency of occurrence of the *DI* values is plotted for different number of iterations (Figure 13). The result shows the convergence of the *DI* distribution when performing 1000 iterations.

The histogram in Figure 14 shows the frequency of occurrence of different damage levels in the tower under the action of the earthquake, defined by the Damage Index (DI). It is possible to appreciate that there is a first peak in the lower-damage zone and another one for *DI* values close to those corresponding to the mean values of the material properties probability distributions. In nearly

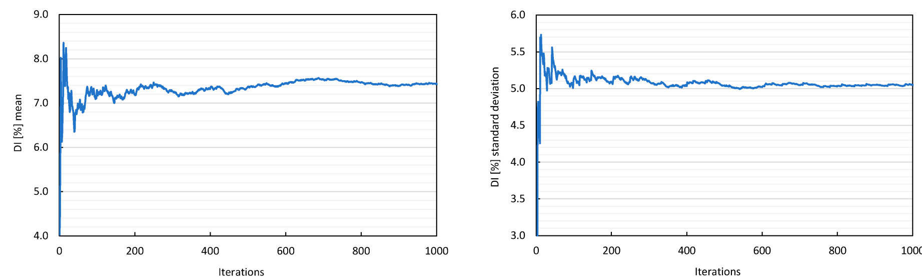

(a) (b)

Figure 12: Convergence analysis for the number of iterations: mean value (a) and standard deviation (b) of the Damage Index (*DI*).

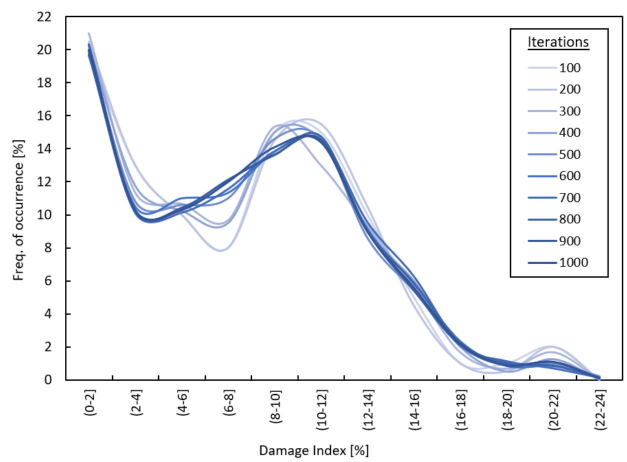

Figure 13: Convergence analysis for the number of iterations: Damage Index distribution.

94 % of the cases, the general damage in the structure can be considered as insignificant (DI $<$ 15 %) and only in about a 6 % of the tests a moderate damage (15 % $\leq$ DI $<$ 25 %) is found. The *DI* is never greater than 25 %, so the structure as a whole would not fail in the event of an earthquake.

However, since the *DI* represents only the overall performance of the structure, it is important to analyze the distribution of stresses and yield zones along the building. As mentioned in the initial analysis for the whole church, there are stress concentrations in the areas where the tower connects with the rigid walls of the church, and in the base of the tambour of the dome (Figure 15). A specific study should be carried out about the stress concentrations and their potential effect on the structural integrity of the tower. Furthermore, when analyzing the results, it should be be born in mind that the assessment of the seismic capacity of a masonry building remains difficult due to the complexity and randomness of the seismic response and the sensitivity of the numerical tools to the input

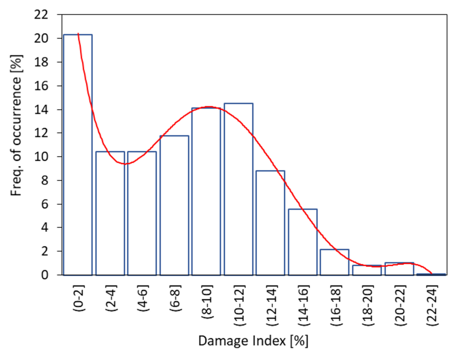

Figure 14: Histogram of the Damage Index in the structure due to the seismic action.

variables [18].

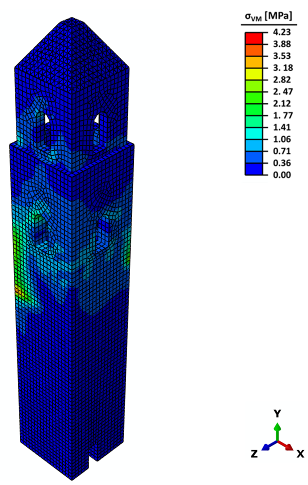

Figure 15: Contour plot of Von Mises stresses in the bell tower under the seismic action.

5.3.1. Influence of the variables in the Damage Index

Another relevant information that can be obtained from the analysis is the relationship between the problem input variables (material properties) and the resulting damage in the building. To this end, the correlation between DI and material properties of the tower walls (travertine) are shown in Figure 16.

It follows from these correlations that the value of the compressive strength does not influence the level of damage due to the earthquake, while the tensile strength seems crucial and perfectly correlated with the DI. These results are consistent with the characteristics of masonry, which shows low tensile strength,

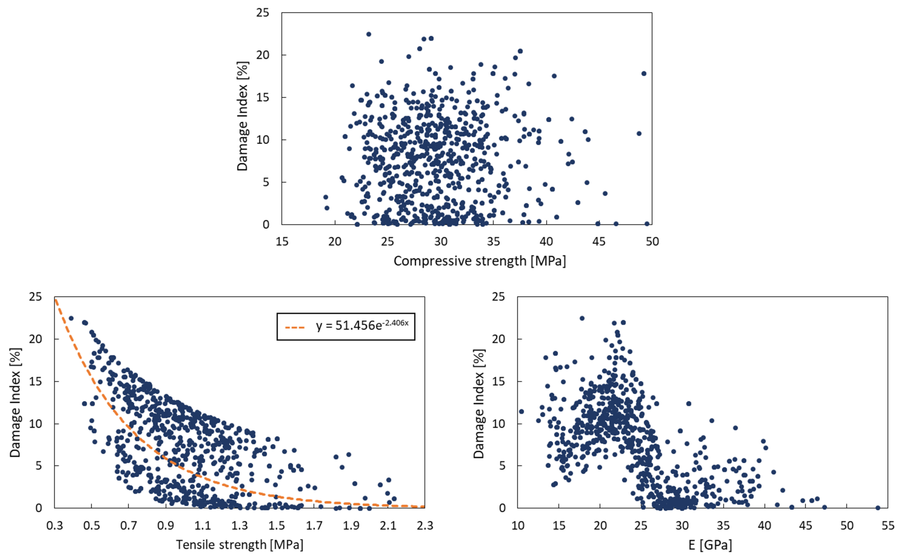

Figure 16: Damage Index as a function of the compressive strength (top), tensile strength (bottom left) and Young's modulus (bottom right).

and also with the effects observed in existing masonry structures damaged by seismic events.

In the case of the Young's modulus, an increase in Young's modulus leads to smaller *DI* values, as might be expected. However, with values of E between 20 GPa and 24 GPa, there is a significant increase in the structural damage. The reason of these abnormal values of the *DI* in this range of Young's modulus values can be found by analyzing the energy spectrum of the earthquake and the vibration modes of the tower. In fact, the energy spectrum of the earthquake (Figure 17) has a peak for both X and Y directions in a frequency very close to the first vibration mode of the building with Young's modulus values within the aforementioned range (ca. 11.4 Hz).

Finally, the *DI* is plotted as a function of the Young's modulus and the tensile stress (Figure 18) in order to analyse the combined effect of these two parameters on the structural damage. The result reveals that for very low values of the tensile strength (lower than approx. 0.6 MPa), a severe damage may occur even for high values of the elastic modulus. It is important to highlight that such low tensile strength values have been reported for masonry structures in some other studies [41, 43]. It can also be observed that, when the Young's modulus takes values over the aforementioned values of resonance, the *DI* radically decreases for every tensile strength value.

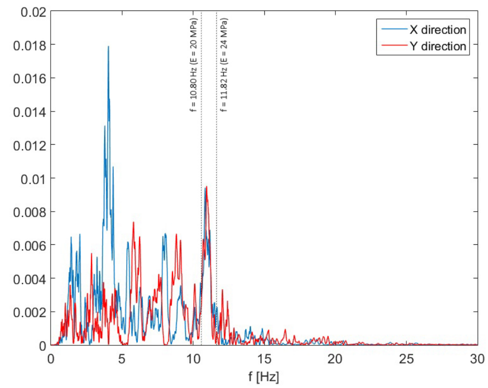

Figure 17: Energy spectrum of the earthquake, X and Y directions.

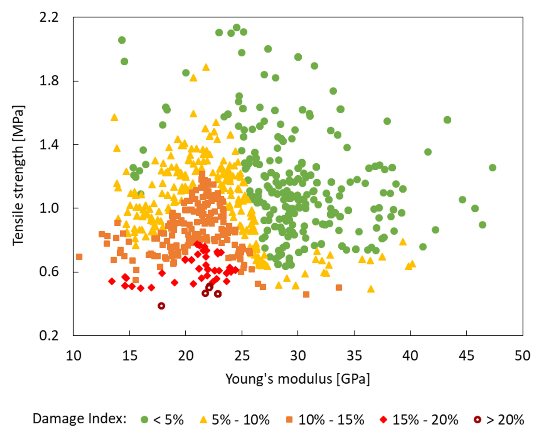

Figure 18: Damage Index as a function of Young's modulus and tensile strength.

6. Conclusions

This paper presents a methodology for a probability-based reliability analysis, in order to asses the damage on a existing masonry structures under seismic actions. This framework is applied to a historical masonry building: the church of San Justo y Pastor located in Granada (Spain).

The probabilistic reliability assessment is based on the consideration of a log-normal probabilistic distribution for the material properties [32], taking into account the uncertainty which is present in the values obtained via a non-destructive technique (SASW). The log-normal random values of the material properties are introduced in a three-dimensional model of the structure developed in a FEM software, where a Monte-Carlo type analysis is carried out. A seismic action in both horizontal directions, with PGA according to the Spanish seismic code [47], is considered as the main action, along with the self-weight of the structure.

The results of the analysis reveal that the bell tower of the church undergoes the greatest displacements and stresses, while the main body of the church behaves as a quasi-rigid body in comparison. The evaluation of a Damage Index (DI), which represents the damaged volume of the church, shows that the structure as a whole is potentially resistant in the event of a earthquake. However, since the *DI* is a measure of the overall performance of the structure, the effects of stress concentration at the junction between the tower and the church walls should be investigated in more detail.

Regarding to the influence of each material property on the structural damage, it is possible to conclude that the *DI* is mainly correlated with the tensile strength and the Young's modulus, and not with the compressive strength at all. It bears to mention that values of E between 20 GPa and 24 GPa bring a significant increase in the structural damage. This abnormal damage is due to the fact that the structure with the mentioned range of E values has its first modal frequency very close to the main frequency of the earthquake, therefore increasing the seismic load absorbed by the structure.

References

[1] A. Rodríguez Gutiérrez de Ceballos, Bartolomé de Bustamante y los orígenes de la arquitectura jesuítica en España, Institum Historicum Societatis Iesus, Rome, 1967.

[2] M. Córdoba Salmerón, Patrimonio artístico y ciudad moderna. el El Conjunto Jesuítico y Colegio de San Pablo entre los siglos XVI y XVIII, Ph.d. thesis, Universidad de Granada, Spain (2005).

[3] Google Maps, Church of San Justo y Pastor, Granada, Spain (2017). URL https://www.google.es/maps/@37.177586,-3.6020191,99a,35y,9.5h,53.76t/data=!3m1!1e3

[4] J. M. Barrios Rozúa, Arquitectura y enseñanza: Los Jesuitas en Granada, in: Las huellas los Jesuit. en Granada. Del Col. San Pablo a la Fac. Teol., Facultad de Teología de Granada, Granada, 2014.

[5] J. A. Llopis Solbes, Proyecto de Obras de Restauración de la Iglesia de los Santos Justo y Pastor de Granada (1981).

[6] M. De Tíscar Ramírez Molina, Análisis estructural de la cúpula de la iglesia de San Justo y Pastor de Granada, Masther thesis, Universidad de Granada, Spain (2012).

[7] T. Aoki, D. Sabia, D. Rivella, T. Komiyama, Structural characterization of a stone arch bridge by experimental tests and numerical model updating, Int. J. Archit. Herit. 1 (3) (2007) 227–250. doi:10.1080/15583050701241208.

[8] F. Martínez Soto, E. Puertas, R. Gallego, F. J. Suarez, Using Spectral Analysis of Surface Waves to characterize construction materials in built Cultural Heritage : The Church of Saint Justo & Pastor, in: 6th Int. Conf. Herit. Sustain. Dev., Vol. 2, Granada, Spain, 2018.
URL https://www.researchgate.net/publication/322065481{_}Using{_}Spectral{_}Analysis{_}of{_}Surface{_}Waves{_}to{_}characterize{_}cor

[9] Joint Committee on Structural Safety, Part 3: Material properties. 3.0 General principles, in: JCSS Probabilistic Model Code, 2000.
URL https://www.jcss.byg.dtu.dk/Publications/Probabilistic{_}Model{_}Code

[10] F. J. Suarez, R. Bravo, Historical and probabilistic structural analysis of the Royal ditch aqueduct in the Alhambra (Granada), J. Cult. Herit. 15 (5) (2014) 499–510. doi:10.1016/j.culher.2013.11.010.

[11] S. E. Chidiac, S. Foo, Guidelines for the seismic assessment of stone-masonry structures, Tech. rep., Public Works & Government Services Canada, Hull, Quebéc (2002). doi:10.13140/2.1.4276.9441.

[12] L. Schueremans, Probabilistic evaluation of structural unreinforced masonry, Phd diss., Katholieke Universiteit Leuven, Belgium (2001).
URL https://lirias.kuleuven.be/handle/123456789/160474

[13] B. G. Jonas, Experiencing Loss, in: B. G. Jonas (Ed.), Prot. Hist. Archit. Museum Collect. from Nat. Disasters, Butterworth-Heinemann, Stoneham, MA, USA, 1986, Ch. SECTION ON, pp. 3–14. doi:https://doi.org/10.1016/B978-0-409-90035-4.50005-4.

[14] U. Rücker, D. W. Hille, D. Rohrmann, F08a Guideline for the assessment of existing structures, in: Federal Institute ofMaterials Research and Testing (BAM) (Ed.), SAMCO, Berlin, Germany, 2006.
URL http://www.samco.org/network/download{_}area/ass{_}guide.pdf

[15] O. Ditlevsen, H. O. Madsen, Structural Reliability Methods, no. July, John Wiley & Sons Ltd, Chichester, 2005.
URL http://www.od-website.dk//index-2.html/books.htm

[16] S. Seyedain Boroujeni, N. Shrive, A reliability assessment methodology for existing masonry structures, in: 13th Can. Mason. Symp., Halifax, Canada, 2017.

[17] P. G. Asteris, On the Structural Analysis and Seismic Protection of Historical Masonry Structures, Open Constr. Build. Technol. J. 2 (1) (2008) 124–133. doi:10.2174/1874836800802010124.

[18] G. de Felice, S. De Santis, P. B. Lourenço, N. Mendes, Methods and Challenges for the Seismic Assessment of Historic Masonry Structures, Int.

J. Archit. Herit. 11 (1) (2017) 143–160. doi:10.1080/15583058.2016.1238976.

[19] E. Giordano, F. Clementi, A. Nespeca, S. Lenci, Damage assessment by numerical modeling of Sant'Agostino's Sanctuary in Offida during the Central Italy 2016-2017 seismic sequence, Front. Built Environ. 4 (January) (2019) 1–17. doi:10.3389/fbuil.2018.00087.

[20] A. Gallego y Burín, Granada : guía artística e histórica, 7th Edition, Editorial Comares S.L., Granada, Spain, 1982.

[21] Ministerio de Cultura, Real Decreto 500/1980, de 25 de enero, por el que se declara monumento histórico-artístico, de carácter nacional, la colegiata de los Santos Justo y Pastor, en Granada (1980).
URL https://www.boe.es/boe/dias/1980/03/20/pdfs/A06251-06251.pdf

[22] J. M. Gómez-Moreno Calera, La arquitectura religiosa granadina en la crisis del Renacimiento (1560-1650), Universidad de Granada, Granada, 1989.

[23] E. Olivares D'Angelo, Historia del Colegio de San Pablo. Granada 1554-1765. Archivo Histórico Nacional. Madrid. Ms. JESUITAS, libro 773. Trascripción de Joaquín de Betancourt S.I., Facultad de Teología de Granada, Granada, Spain, 1991.

[24] A. M. García Marín, Comparación de modelos numéricos y experimentales de propagación de ondas, Bachelor thesis, Universidad de Granada, Spain (2017).

[25] Universidad de Granada, Ruta GEOdidáctica por monumentos de la ciudad de Granada (2012).

[26] ACI Committee 318, 318-19 Building Code Requirements for Structural Concrete, Tech. rep. (2019).
URL https://www.concrete.org/store/productdetail.aspx?ItemID=318U19{&}Language=English{&}Units=US{_}Units

[27] Comité ACI 318, ACI 318S-14 Requisitos de Reglamento para Concreto Estructural, Tech. rep., American Concrete Institute, Farmington Hills, MI, U.S.A. (2014).

[28] ACI Committee 363, 363R-10 Report on High-Strength Concrete, Tech. rep., American Concrete Institute, Farmington Hills, MI, U.S.A. (2010).

[29] CEN, EN 1992-1-1. Eurocode 2: Design of concrete structures - Part 1-1 : General rules and rules for buildings (2004).

[30] H. Yildirim, O. Sengul, Modulus of elasticity of substandard and normal concretes, Constr. Build. Mater. 25 (4) (2011) 1645–1652. doi:10.1016/j.conbuildmat.2010.10.009.

[31] ASCE, FEMA 356 Prestandard November 2000, no. November, Federal Emergency Management Agency, Washington, D.C., 2000.

[32] C. A. Graubner, E. Brehm, Part 3: Resistance models. 3.2 Masonry properties, in: JCSS Probabilistic Model Code, 2011. doi:10.4324/9780203362402.ch3.

[33] A. Ferrante, F. Clementi, G. Milani, Advanced numerical analyses by the Non-Smooth Contact Dynamics method of an ancient masonry bell tower, Math. Methods Appl. Sci. (June 2019) (2020) 1–20. doi:10.1002/mma.6113.

[34] V. N. Moreira, J. Fernandes, J. C. Matos, D. V. Oliveira, Reliability-based assessment of existing masonry arch railway bridges, Constr. Build. Mater. 115 (2016) 544–554. doi:10.1016/j.conbuildmat.2016.04.030.

[35] J. M. Tamborero del Pino, A. Cejalvo Lapeña, NTP 418 : Fiabilidad : la distribución lognormal (1994).

[36] P. G. Asteris, M. G. Douvika, M. Apostolopoulou, A. Moropoulou, Seismic and restoration assessment of monumental masonry structures, Materials (Basel). 10 (8) (2017) 895. doi:10.3390/ma10080895.

[37] P. Roca, M. Cervera, G. Gariup, L. Pela', Structural analysis of masonry historical constructions. Classical and advanced approaches, Arch. Comput. Methods Eng. 17 (3) (2010) 299–325. doi:10.1007/s11831-010-9046-1.

[38] Dassault Systèmes, 23.6.3 Concrete damaged plasticity (2013).
URL http://130.149.89.49:2080/v6.13/books/usb/default.htm

[39] M. Annecchiarico, F. Portioli, R. Landolfo, Micro and macro-finite element modeling of brick masonry panels subject to lateral loadings, COST ACTION C26 Urban Habitat Constr. under Catastrophic Events - Proc. Final Conf. (2010) 315–320.

[40] G. Castellazzi, A. M. D'Altri, S. de Miranda, F. Ubertini, An innovative numerical modeling strategy for the structural analysis of historical monumental buildings, Eng. Struct. 132 (2017) 229–248. doi:10.1016/j.engstruct.2016.11.032.

[41] G. Milani, M. Valente, C. Alessandri, The narthex of the Church of the Nativity in Bethlehem: A non-linear finite element approach to predict the structural damage, Comput. Struct. 207 (2018) 3–18. doi:10.1016/j.compstruc.2017.03.010.

[42] M. Valente, G. Milani, Damage assessment and partial failure mechanisms activation of historical masonry churches under seismic actions: Three case studies in Mantua, Eng. Fail. Anal. 92 (June) (2018) 495–519. doi:10.1016/j.engfailanal.2018.06.017.

[43] M. Valente, G. Milani, Damage assessment and collapse investigation of three historical masonry palaces under seismic actions, Eng. Fail. Anal. 98 (January) (2019) 10–37. doi:10.1016/j.engfailanal.2019.01.066.

[44] G. Fortunato, M. F. Funari, P. Lonetti, Survey and seismic vulnerability assessment of the Baptistery of San Giovanni in Tumba (Italy), J. Cult. Herit. 26 (2017) 64–78. doi:10.1016/j.culher.2017.01.010.

[45] N. D. Agüera, M. E. Tornello, C. D. Frau, Structural Response of Unreinforced Masonry Walls, J. Civ. Eng. Archit. 10 (2016) 219–231. doi:10.17265/1934-7359/2016.02.011.

[46] D. Giardini, J. Woessner, L. Danciu, G. Valensise, G. Grünthal, F. Cotton, R. Pinho, The SHARE Consortium, European Seismic Hazard Map for Peak Ground Acceleation, 10% Exceedance Probabilities in 50 years (2013). doi:10.2777/30345.

[47] Ministerio de Fomento, NCSE-02 Norma de Construcción Sismorresistente: Parte general y edificación (2009).
URL http://www.060.es

[48] M. Navarro, A. García-Jerez, F. Vidal, M. Feriche, T. Enomoto, G. Alguacil, Análisis de los efectos de sitio en la ciudad de Granada (sur de España) a partir de medidas de ruido ambiental (2011).

[49] J. Woessner, D. Laurentiu, D. Giardini, H. Crowley, F. Cotton, G. Grünthal, G. Valensise, R. Arvidsson, R. Basili, M. B. Demircioglu, S. Hiemer, C. Meletti, R. W. Musson, A. N. Rovida, K. Sesetyan, M. Stucchi, The 2013 European Seismic Hazard Model: key components and results, Bull. Earthq. Eng. 13 (12) (2015) 3553–3596. doi:10.1007/s10518-015-9795-1.

[50] F. Clementi, A. Ferrante, E. Giordano, F. Dubois, S. Lenci, Damage assessment of ancient masonry churches stroked by the Central Italy earthquakes of 2016 by the non-smooth contact dynamics method, Bull. Earthq. Eng. 18 (2) (2020) 455–486. doi:10.1007/s10518-019-00613-4.